



Published in final edited form as:

DNA Repair (Amst). 2019 May ; 77: 76–86. doi:10.1016/j.dnarep.2019.03.004.

Mechanisms underlying aflatoxin-associated mutagenesis – Implications in carcinogenesis

Amanda K. McCullough^{a,b}, R. Stephen Lloyd^{a,b,c,*}

^aOregon Institute of Occupational Health Sciences, Oregon Health & Science University, Portland, OR 97239, United States

^bDepartment of Molecular and Medical Genetics, Oregon Health & Science University, Portland, OR 97239, United States

^cDepartment of Physiology and Pharmacology, Oregon Health & Science University, Portland, OR 97239, United States

Abstract

Chronic dietary exposure to aflatoxin B₁ (AFB₁), concomitant with hepatitis B infection is associated with a significant increased risk for hepatocellular carcinomas (HCCs) in people living in Southeast Asia and sub-Saharan Africa. Human exposures to AFB₁ occur through the consumption of foods that are contaminated with pervasive molds, including *Aspergillus flavus*. Even though dietary exposures to aflatoxins constitute the second largest global environmental risk factor for cancer development, there are still significant questions concerning the molecular mechanisms driving carcinogenesis and what factors may modulate an individual's risk for HCC. The objective of this review is to summarize key discoveries that established the association of chronic inflammation (most commonly associated with hepatitis B viral (HBV) infection) and environmental exposures to aflatoxin with increased HCC risk. Special emphasis will be given to recent investigations that have: 1) refined the aflatoxin-associated mutagenic signature, 2) expanded the DNA repair mechanisms that limit mutagenesis via adduct removal prior to replication-induced mutagenesis, 3) implicated a specific DNA polymerase in the error-prone bypass and resulting mutagenesis, and 4) identified human polymorphic variants that may modulate individual susceptibility to aflatoxin-induced cancers. Collectively, these investigations revealed that specific sequence contexts are differentially resistant against, or prone to, aflatoxin-induced mutagenesis and that these associations are remarkably similar between in vitro and in vivo analyses. These recent investigations also established DNA polymerase ζ as the major polymerase that confers the G to T transversion signature. Additionally, although the nucleotide excision repair (NER) pathway has been previously shown to repair aflatoxin-induced DNA adducts, recent murine data demonstrated that NEIL1-initiated base excision repair was significantly more important than NER relative to the removal of the highly mutagenic AFB₁-Fapy-dG adducts. These data suggest that inactivating polymorphic variants of NEIL1 could be a potential driver of HCCs in aflatoxin-exposed populations.

*Corresponding author at: Oregon Institute of Occupational Health Sciences, Oregon Health & Science University, Portland, OR 97239, United States. lloydst@ohsu.edu (R.S. Lloyd).

Conflict of interest

The authors declare that there are no conflicts of interest.

Keywords

DNA repair; DNA replication; NEIL1; Polymerase zeta; Hepatocellular carcinoma

1. Introduction

1.1. Discovery and acute toxicities

Aflatoxins are a group of closely-related chemical structures that are produced by fungal strains of *Aspergillus flavus* and *Aspergillus paraciticus* (reviewed in [1,2]). The discovery of the biological importance of aflatoxins dates to the late 1950s and early 1960s when they were identified as the causative agent(s) associated with large numbers of poultry (turkey poults, ducklings, and chicks) deaths described as “turkey X” syndrome. The source of this acutely-toxic exposure was identified as *A. flavus* contaminated peanut meal [3–5]. These investigations were corroborated using *A. flavus*-contaminated nut extracts to induce liver toxicity in ducklings and liver cancer in rats. Acute toxicities from ingestion of foods contaminated with *A. flavus* or *A. paraciticus* are not limited to these species, but include humans in which outbreaks of acute aflatoxicosis are documented, with symptoms including vomiting, abdominal pain, pulmonary edema, fatty liver, liver necrosis and potential death (reviewed in [1]). These geographically-localized outbreaks have been documented in India, Kenya, and Malaysia in which fungal-contaminated corn was the common source of the acute toxicity and deaths. However, corn is not the only food stuff that can routinely be contaminated with these molds but includes peanuts, milo, sorghum, copra, and rice [2]. Overall, the world-wide burden of aflatoxin exposure was previously estimated to affect ~5 billion people (reviewed in [6]) and this estimate is likely to underestimate current population exposures. However, systematic efforts to reduce aflatoxin exposures in China through food policy reforms to minimize maize and maximize rice consumption have greatly reduced primary liver cancers and biomarkers of aflatoxin exposure [7,8]. The reductions in HCCs are also the manifestation of comprehensive efforts toward universal vaccination against hepatitis B virus (HBV) in China [7,9].

1.2. Biomarkers of exposure

Although the severity of symptoms associated with acute aflatoxicosis highlights the short-term dangers associated with ingestion of foods contaminated with these molds, the scope of the adverse human health effects from routine consumption of foods contaminated with sub-acute levels of aflatoxins affects orders of magnitude more humans than compared to those who experience acute disease. To understand these relationships, it was necessary to develop aflatoxin-associated biomarkers of human exposure, geographic mapping of aflatoxin-producing molds and other potential contributing etiological factors such as chronic inflammation due to hepatitis B and C viral (HBV and HCV) infections and alcohol consumption with liver disease and HCCs.

To establish biomarkers of exposure, it was necessary to determine the structures of the aflatoxins that are produced by various strains of these molds, understand the bioactivation and detoxification pathways, characterize a subset of biologically relevant macromolecules modified by activated aflatoxins, and develop ultra-high sensitivity assays to quantitate these

modified end-product macromolecules. The core structure of the four aflatoxins produced by *A. flavus* is a substituted coumarin, linked to a dihydrofuran moiety and are designated AFB₁, AFB₂, AFG₁, and AFG₂. The “B” abbreviation designates structures with a blue fluorescence, while the “G” denotes green fluorescence. The toxigenic strains of *A. flavus* produce AFB₁, the most common and abundant form of aflatoxin and has the greatest carcinogenic potential (reviewed in [1,2]). Thus, AFB₁ has been the most extensively studied of these molecules in terms of metabolic pathways, biomarkers of exposure, mutagenic and carcinogenic analyses.

As ingested, AFB₁ is not reactive with other cellular macromolecules such as DNA, RNA or proteins. In the liver, AFB₁ undergoes either hydroxylation to molecules that are not associated with carcinogenesis or oxidation at the 8, 9 position to form both the exo- and endo- epoxides that have significant biological impacts (reviewed in [10]). The liver cytochrome P450 that is predominantly responsible for this bioactivation is CYP3A4 [11], with potential contributions from CYP3A5 [11,12], CYP3 A7 and CYP1A2 (predominantly extra-hepatic).

The cellular environment to process the AFB₁ 8,9 exo-epoxide is critical for determining subsequent biological impacts of aflatoxin exposures. Detoxification pathways primarily involve conjugation via reaction with glutathione S-transferases and potential contributions of microsomal epoxide hydrolase (reviewed in [13,14]). It is the knowledge of the bioactivation and detoxification pathways that has identified strategies for the design of chemoprevention trials to reduce or prevent aflatoxin-associated HCCs. Specifically, the upregulation of detoxification pathways has been the subject of intensive investigations since efforts to tip the balance toward inactivation of the aflatoxin epoxide is strongly anticipated to decrease DNA lesion burden and subsequent mutagenic and carcinogenic outcomes [15–17]. The fundamental design of dietary interventions (such as routine consumption of sulforaphane via broccoli or broccoli sprouts) in aflatoxin-associated HCC is based on transcriptional upregulation through Keap1-Nrf2-ARE signaling (reviewed by [1,18]). The molecular basis for this intervention is based on the binding of sulforaphane with Keap1, which in turn disrupts poly ubiquitinated-mediated proteasomal degradation of Nrf2. Maintaining elevated levels of Nrf2 allows for enhanced transcription of Nrf2 target genes that confer cytoprotective responses and suppress carcinogenesis.

1.3. In utero exposures - biological significance

The balance between inactivation of the aflatoxin epoxides as glutathione conjugates and formation of DNA adducts is also a critical issue for *in utero* exposures. Due to the pervasiveness of aflatoxin exposures in many portions of the world, it is of critical importance to understand the potential for adverse effects on fetal development and long-term susceptibility to early onset HCCs. Smith et al have reviewed 10 human and 17 animal cross-sectional studies regarding aflatoxin exposures and adverse birth outcomes and anemia [19]. In humans, a fetal form of CYP3 A4 can be found within 2 months of conception and thus, following maternal ingestion of aflatoxin and transplacental transport, the developing fetus has the potential to activate aflatoxins to the 8,9 epoxide. This bioactivation, coupled with reduced levels of *in utero* glutathione-S-transferases, could significantly increase the

fetal burden of DNA adducts. These human investigations are consistent with *in utero* investigations in mice in which AFB₁ metabolism favors increased DNA damage during fetal development [20]. These increased DNA adduct levels in mice during fetal exposures also translated to increased mutagenesis in 10-week-old animals, in which mutation frequencies in mice exposed to aflatoxin *in utero* were up to 20-fold higher than the adult [21]. These data highlight and reinforce the need to minimize human exposures, especially during pregnancy.

1.4. HBV infection as the primary driver of HCCs - the role of chronic inflammation

Numerous epidemiologic studies have established overwhelming evidence correlating increased risk of developing HCC with chronic HBV infection and this risk ratio has been reported to range from 6- to ~100-fold in carriers vs non-infected [22]. Further, the probability of developing HCCs is well correlated with the relative stage of the disease. These conclusions are strongly reinforced in a recent study that reports a 25-year prospective analysis of HBV infection and HCC in Qidong, China [23]. This study followed a total of approximately two thousand individuals with either positive or negative hepatitis B surface antigen (HBsAg). The ratio of HCC incidence was 12.3 in HBsAg positive versus negative populations and this ratio increased to 28.1 when comparisons were made between individuals who were both HBsAg positive and hepatitis B e antigen (HBeAg) positive relative to negative controls.

In addition to the relative extent of HBV-induced disease progression being a predictor of HCC onset, mutations in the HBV DNA genome are also known to modulate HCC risk ratios. Previously, a double mutation in the HBV basal core promoter (A1762T/G1764A) was found to be associated with increased risk in HCC formation (reviewed in [24]). Although the above-mentioned 25-year retrospective cohort did not confirm that this double-mutation was sufficient to produce statistically significant associations with HCC development, addition of mutations at positions 1766 and 1768 significantly elevated risk ratios, under-scoring the importance of DNA variants in HBV-associated disease.

The combined effects of HBV infection and aflatoxin exposures on the risk for developing HCCs has been rigorously documented in HCC patients and control populations in southern China [25]. In this study, biomarkers of HBV, aflatoxin and oxidative stress (as measured by AFB₁-albumin adducts and protein carbonyl content) were significantly higher in HCC patients relative to age, gender, and HBV serotype-matched groups. These data suggest a strong correlation between HBV infection and oxidative stress in combination with aflatoxin exposures. Further stratification of HCC patients in Guangxi, China relative to HBV status and aflatoxin exposure revealed that there are regions of chromosomal alterations (both gain and loss), effecting copy numbers of oncogenes, tumor suppressor genes and genes associated with drug metabolism and detoxification pathways. [26]. This study also reported strong correlations of aflatoxin-associated HCCs and elevated levels of aldo-keto reductase family 1 member B10 (AKR1B10), an enzyme frequently over-expressed in many solid tumors; however, the mechanism underlying this relationship has not yet been elucidated. In addition to establishing the interrelationships of HBV infection and oxidative stress in HCC

causation, similar correlations have been established for the role and dose response of aflatoxin exposure for increased risk of cirrhosis and cirrhotic HCC [27].

2. AFB₁ DNA adducts

Following ingestion and activation by liver microsomal enzymes, the intermediate AFB₁-epoxide intercalates in duplex DNA on the 5' side of guanine and can form a covalently-bound adduct at N7 guanine, yielding the *trans*-8,9-dihydro-8-(N7-guanyl)-9-hydroxy-aflatoxin B₁ adduct, (AFB₁-N7-dG) (Fig. 1A) [28–30]. Kinetic analyses of the formation and disappearance of AFB₁-DNA adducts revealed that about 20% of the initial, quantitatively abundant, cationic AFB₁-N7-dG lesions are converted to the ring-opened *trans*-8,9-dihydro-8-(2,6-diamino-4-oxo-3,4-dihydropyrimid-5-yl-formamido)-9-hydroxy aflatoxin B₁ (AFB₁-Fapy-dG) adduct (Fig. 1B) within 24 h after a single dose, while the remainder of the N7 adducts underwent spontaneous depurination. Thus, the AFB₁-Fapy-dG adducts become the dominant DNA damage detected in cellular DNA 72 h post exposure, comprising up to 80% of all known AFB₁-induced lesions [31]. Recent investigations have significantly improved measurements of aflatoxin-induced base adducts, including AFB₁-N7-Gua and both diastereomers of AFB₁-Fapy-Gua using liquid chromatography-tandem mass spectrometry [32]. Assay optimization was conducted on DNAs derived from mouse livers in which mice had been treated with AFB₁ in DMSO or DMSO controls. These analyses also revealed a significant aflatoxin-mediated accumulation of (5'R)- and (5'S)-8,5'-cyclo-2'-deoxyadenosines, thus reinforcing the potential for aflatoxin exposures to increase oxidatively-induced DNA damage.

The chemical stability of the AFB₁-Fapy-dG adduct is consistent with the long half-lives of many ring-fragmented purines. The persistence of the AFB₁-Fapy-dG adduct in cells can be at least partially attributed to its intercalation into duplex DNA as detected by NMR and consequent stabilization of the DNA as measured by increased melting temperature [33]. The AFB₁-Fapy-dG adduct is in a chemical equilibrium between α and β deoxyribose anomers [34], with the β -anomer favored in duplex DNA and the α -anomer favored in ssDNA.

3. Mutagenic potential of AFB₁ DNA adducts

3.1. Prokaryotic mutagenesis

A variety of experimental designs have been utilized in bacterial systems to evaluate the mutagenic potential of metabolically activated AFB₁ [35–37]. Mutation frequencies and spectra were established for both the AFB₁-N7-dG adduct and the AFB₁-Fapy-dG structural mixture [37] and estimates of replication blockage were inferred from viral progeny yields. Using site-specifically modified DNAs that were engineered into a single-stranded M13mp7 shuttle vector and replicated in SOS-induced *Escherichia coli*, it was determined that the AFB₁-N7-dG adduct was weakly mutagenic (4%), while the mutagenic potential of AFB₁-Fapy-dG adducts was 32%. The mutation spectra were dominated by G to T transversions, highly consistent with the mutation spectra found in tumors associated with aflatoxin exposures. The yield of replicated M13mp7 progeny showed that the single-stranded shuttle vectors containing the AFB₁-N7-dG adduct was ~100-fold higher than the comparable Fapy

adduct. Bypass of the AFB₁-Fapy-dG containing vectors was highly dependent on the inducible expression of the UmuCD complex, DNA polymerase V.

3.2. Eukaryotic mutagenesis

Molecular epidemiological studies have revealed a prevalent mutation hot spot at codon 249 in TP53 (AGG to AGT) yielding a coding change of R249S in ~50% of HCCs in regions of the world with high HBV infection and aflatoxin exposures [38–40]. Strikingly, this specific mutation is not abundant in other cancers or in portions of the world with minimal aflatoxin exposures [41–45]. Further stratification of HBV-associated HCCs with regard to aflatoxin risk revealed that this specific G to T transversion was strongly associated with aflatoxin exposure [43,45]. Consistent with these data, when cultures of mouse embryo fibroblasts (MEFs) that were harboring multiple copies of a mutation reporter gene, the *cII* transgene, and were treated with activated AFB₁, G to T transversions dominated the mutation spectra, with two of the reporting sequence contexts being identical to the 249 codon of TP53 [46]. Similarly, data derived from using a rat *lacI* transgenic model with aflatoxin exposure showed an ~20-fold increase in mutation frequency that was dominated by G to T transversions [47]. However, in addition to G to T transversions, significant increases in G to A transitions were reported using a double-stranded shuttle vector, pS189, that had been reacted with the activated aflatoxin epoxide [48]. These data also demonstrated that there was not a one-to-one correspondence between the level of adducts at a specific site and the mutation frequencies and that NER repair-deficient cells were more mutation prone.

In addition to these random non-targeted mutagenesis studies, the mutagenic potential of the site-specific N7 cationic AFB₁ and AFB₁-Fapy-dG adducts have also been determined by engineering these adducts into oligodeoxynucleotides and introducing them into single-stranded pMS2 DNA [49]. Following replication of both control and modified DNAs in COS-7 cells, and subsequent evaluation of mutagenic replication, these data showed that the cationic AFB₁-N7-dG adduct had an overall mutation frequency of 45% with > 80% of these mutations being G to T [50]. The mutation spectra for AFB₁-Fapy-dG were 86% G to T, 8% G to A, and the remaining 6% a mixture of G to C and single nucleotide deletions [49]. The mutation frequency associated with replication bypass of the AFB₁-Fapy-dG adduct was exceptionally high (> 97%); to the best of our knowledge, this mutation frequency is the highest of any known carcinogen.

4. Translesion synthesis of aflatoxin DNA adducts

In addition to elucidating the mutation spectra and frequencies for the N7-AFB₁-dG and AFB₁-Fapy-dG adducts, studies were also conducted to assess which DNA polymerases might be able to catalyze translesion DNA synthesis past these adducts [49,50]. Since the shuttle vector data had shown that N7-AFB₁-dG adduct was accurately by-passed in > 50% of replication events in ssDNA, it was important to ascertain which polymerase(s) had the capacity to incorporate and extend a dC opposite the lesion. Although DNA adducts as large as aflatoxin were anticipated to be complete blocks to replicative polymerases, DNA polymerase delta (*pol δ*) was able to replicate past the N7-cationic species, albeit at greatly reduced efficiencies [50]. This bypass was dominated by error-free incorporation of dC.

Further analyses using DNA polymerase zeta, kappa, eta, and iota (pol ζ , pol κ , pol η , pol ι , respectively) were conducted. DNA pol ζ preferentially incorporated the correct dC opposite the lesion with less efficient insertions of dA, dG and dT. Pol κ displayed no preferential incorporation of any of the dNTPs, while pol η preferentially incorporated dA and dG. Pol ι preferentially incorporated dC and dT. pol ζ and pol ι preferentially extended a correct dC opposite the adduct, while pol η and pol κ extended both matched and mismatched primers. Overall, these data suggest that pol ζ , pol ι , and replicative polymerases such as pol δ could be responsible for error-free bypass and extension of N7-AFB₁-dG adducts, while pol κ and pol η may be sufficient to generate the G to T and G to A mutations.

In contrast to the complex picture of incorporation and extension past the N7-AFB₁-dG adduct, studies examining replication of DNAs containing a site-specific AFB₁-Fapy-dG adduct showed that pol ζ was likely the only polymerase that could conduct translesion DNA synthesis [49]. In accord with the mutagenesis data from *in vitro* cell culture, animal models, and human tumors, pol ζ preferentially incorporated dA opposite the ring-opened aflatoxin adduct and would only extend from a mismatched dA. These data suggested that there may be an exclusive role for pol ζ in bypass of the AFB₁-Fapy-dG adduct.

Based on the biochemical data identifying a predominant/unique role for pol ζ in replication past AFB₁-Fapy adducts, it was hypothesized that cells deficient in this polymerase would be very sensitive to the cytotoxic effects of exposure to aflatoxin. To test this hypothesis, isogenic pol ζ -deficient (*Rev3L*^{-/-}), -proficient (*Rev3L*^{+/-}), and human *Rev3L* complemented (*Rev3L*^{-/-} + *hRev3L*) mouse embryonic fibroblasts [51–56] were treated with AFB₁ that had been activated with rat liver microsomes [57]. These SV40 TAG-immortalized cells were assayed for growth inhibition by measuring ATP levels or cell death measured by annexin V staining after AFB₁ treatment (Fig. 2A, B). In a dose-dependent manner, the *Rev3L*^{-/-} MEFS were significantly more sensitive to aflatoxin challenge than either *Rev3L*^{+/-} or *Rev3L*^{-/-} + *hRev3L*.

To gain insights into whether growth inhibition occurred rapidly as a result of AFB₁-induced DNA adducts or was driven by residual adduct-induced replication collapse, cells were exposed to activated AFB₁ and analyzed after 18 h by flow cytometry using annexin V with propidium iodide dual staining. Consistent with a model that the differential sensitivity of *Rev3L*^{-/-} and *Rev3L*^{+/-} cells to aflatoxin treatment requires subsequent rounds of DNA replication, both cells displayed no significant differences in annexin V staining post AFB₁ exposure. These data suggested that growth inhibition may manifest following subsequent replication, accumulation of DNA damage, and alteration of cell cycle checkpoint control.

This prediction was experimentally tested and substantiated by treating pol ζ -proficient and deficient cells with activated AFB₁ and using flow cytometry to measure arrest at specific cell cycle stages [57]. In comparison to *Rev3L*^{+/-} cells, *Rev3L*^{-/-} MEFS showed a significant change in cell cycle distribution 24 h post treatment with *Rev3L*^{-/-} cells accumulating in late S and G2/M phases. At the dose of AFB₁ used, no change in cell cycle profile was detected in *Rev3L*^{+/-} cells. Further, using BrdU pulse labeling for 1 h prior to AFB₁ treatment and subsequent release, *Rev3L*^{+/-} cells showed no G2/M arrest, while *Rev3L*^{-/-} cells exhibited increased populations of cells in late S and G2/M. These data

suggested that sites of unrepaired AFB₁-Fapy-dG lesions could create gaps in the completion of replication which upon further DNA synthesis could induce double-stranded DNA breaks.

To determine whether AFB₁ treated *Rev3L*^{-/-} MEFS accumulated increased numbers of dsDNA breaks relative to *Rev3L*^{+/-} cells, levels of γ -H2AX foci were determined over 72 h post exposure [57]. While the number of γ -H2AX positive cells in *Rev3L*^{+/-} MEFS peaked at 24 h and returned to initial levels by 72 h (Fig. 3A, B), *Rev3L*^{-/-} MEFS contained high basal levels of γ -H2AX and were never able to resolve the AFB₁-induced increases in γ -H2AX foci over 72 h. Consistent with these data, pol ζ deficient cells displayed increased levels of micronuclei and multi-nucleated cells relative to the pol ζ -proficient counterparts (Fig. 3C–F, respectively).

Given these results, it was anticipated that mitotic catastrophe, as defined by the premature entry of severely damaged cells from G2 into metaphase, could be the mechanism of induced cell death. Although *Rev3L*^{-/-} cells have increased spontaneous chromosomal instability, chromosome gaps and breaks [51,55] when treated with activated AFB₁, *Rev3L*^{-/-} cells showed significantly increased radials and breaks (Fig. 3G and H, respectively). Overall, for murine models these data reveal a unique role for pol ζ in the bypass of AFB₁-induced DNA adducts, suggesting that no other polymerases can efficiently substitute in these incorporation and extension translesion synthesis steps.

5. Signature 24- the aflatoxin signature

The identification of mutagenic signatures that are associated with specific environmental or chemotherapeutic exposures represents a major milestone in understanding the etiology of human cancers, with The Cancer Genome Atlas serving as a repository of these data. Even though prior investigations had correlated dietary aflatoxin exposures with G to T mutations in p53 [38,39], exome sequencing analyses of a total of 243 human HCCs revealed a distinctive aflatoxin (and HBV) signature assigned Signature 24 [58]. This designation was based on liver tumors and control non-tumor liver tissue that had been surgically resected from patients in three European countries in which the tumors were associated with cirrhosis, fibrosis, or non-fibrotic livers with risk factors including alcohol intake, HCV, non-alcoholic steatohepatitis concomitant with metabolic syndrome, HBV and hemochromatosis. Hierarchical cluster analysis revealed a total of 6 individual mutational signatures that were significantly associated with demographic, etiologic, and molecular characteristics. Their analyses revealed that one of these molecular signature groups had a high rate of G to T (C to A) transversions and that all patients within this cluster were migrants who were born in subtropical African countries and infected with HBV. These data formed the basis of defining an aflatoxin-specific signature, designated Signature 24.

Recent independent investigations have discovered that specific DNA sequence contexts greatly influence the final mutation signature (see recent review by [59]). Even though Signature 24 is defined as predominantly G to T transversions, with ~10% G to A transitions, the first conclusive evidence that not all trinucleotide sequence contexts involving dG were equally susceptible to mutation, was generated in the laboratory of Dr.

John Essigmann [60]. Utilizing the *gpt* B6C3 F1 mouse model, newborn mice were treated with AFB₁, livers harvested at 10 and 72 weeks, and *gpt* DNA isolated and analyzed by Next Generation sequencing. The depth of the sequencing allowed for the discovery that at 10 weeks post-AFB₁ treatment, among the sequence contexts with at least one G, mutagenic hot spots were predominantly at CGC and to a lesser degree CGG. Equally notable in their data were sequence contexts that appeared to be refractory to mutation. Although there was a dominant Signature 24 at 10 weeks in the liver, comparable analyses at 72 weeks showed that while non-tumor liver tissues maintained a strong AFB₁ signature, sequence analyses of tumor DNAs revealed a significant dilution of the AFB₁ signature presumably reflecting oxidative stress.

Shortly after this study was published, Dr. Steve Rozen's group using cell culture lines, HepaRG and HepG2, and two mouse models, wild type (WT) C57B16 and transgenic mice expressing HBsAg also reported distinct expanded signatures, with hot spots primarily detected at TGC, AGC, and TGG sites [61]. Their analyses included examination of whether mutations were in the transcribed versus non-transcribed stands with mutations preferentially found in the non-transcribed strand. These studies also showed a significant decrease in mutagenesis near the 5' end of actively transcribed genes and increased mutagenesis in late replicating genomic regions. These data suggest a significant influence of transcription-coupled repair in limiting mutagenesis.

Having established commonalities in *in vitro* and *in vivo* mutation signatures, they integrated these results with recent genomic sequencing of HCC tumors from patients in Qidong China [62] and publicly accessible mutation spectra from individuals with HCCs and probable aflatoxin exposure. Using principle component analyses they were able to further extend the aflatoxin-induced mutation signature.

Collectively, these data demonstrate that all sequence contexts are not equally susceptible to AFB₁-induced mutagenesis. Theoretically, there are several mechanisms that could significantly influence the final observed sequence context-dependent hot and cold spots. The following factors could contribute to developing a mechanistic understanding: 1) sequence context effects on the initial formation of N7-AFB₁-dG, 2) sequence context effects on the relative proportion of abasic site formation versus ring-opening of the AFB₁-Fapy-dG adduct, 3) structural conformation differences in varying sequence contexts, 4) differences in rates and efficiencies of either nucleotide excision repair (NER) or base excision repair (BER), and 5) differential fidelity of polymerase ζ (or other replicative or translesion synthesis polymerases) in the bypass of AFB₁. Ongoing investigations will be required to establish the relative contribution of these factors to the mutation signature.

6. Nucleotide excision repair of aflatoxin-induced DNA adducts

As with bulky adducts, such as those created through covalent binding of polycyclic aromatic hydrocarbons, and significant helix distorting modifications, including UV-induced cyclobutane pyrimidine dimers and pyrimidine-pyrimidone 6-4 photoproducts, the AFB₁-induced adducts are subject to repair by NER. This was initially described by the Essigmann group using site-specifically modified oligodeoxynucleotides engineered into vectors for

replication in *E. coli* [63]. These data revealed an essential role for NER in the repair of both adducts, even in the absence of an SOS-induced state. These data confirmed previous studies in which the purified and reconstituted UvrABC complex bound and incised DNAs containing either of the AFB₁ adducts with similar efficiencies [64].

Consistent with the data generated in prokaryotic systems, both AFB₁-induced adducts are repaired by NER in mammalian cells. The involvement of NER in the removal AFB₁-N7-dG in human cells is evident since more adducts accumulate in NER-deficient xeroderma pigmentosum group A (XPA) cells relative to NER-proficient fibroblasts 48 h post treatment [65]. The conclusions were corroborated using nuclear extracts of rat or mouse livers in *in vitro* incision and repair synthesis assays on plasmids containing AFB₁-N7-dG adducts [66]. In addition, XPA^{-/-} mice are somewhat more susceptible to HCC formation relative to WT mice following a single neonatal challenge with AFB₁ [67]. As mentioned above, there was also a strong mutagenic strand bias in both cells (HepG2 and HepaRG) and mouse or human tumors that had been exposed to AFB₁ in which the non-transcribed strand was far more likely to contain mutations than the transcribed strand [61]. Their data also demonstrated that this mutagenic strand bias was closely related to the relative transcriptional activity of individual genes and the relative 5' and 3' position. Collectively, these data suggest a role for transcription-coupled NER in limiting mutagenesis.

Additionally, a crucial role for human NER in protection from aflatoxin-induced HCCs has been discovered through molecular epidemiological analyses of individuals carrying polymorphisms in either the XPC or XPD genes [68,69]. Both studies revealed dramatic increases in odds ratios for HCC formation in homozygous variants (Lys751Gln in XPD and Lys939Gln in XPC), with long duration and high concentration AFB₁ exposures. However, only modest increases were observed in individuals heterozygous for these alleles. Based on analyses of transcriptional strand bias mutagenesis in murine and human tumors, it can be inferred that NER transcription-coupled repair is operative in limiting mutations (58–61).

7. Base excision repair of AFB₁-Fapy-dG adducts

Although there are convincing data that confirm DNA repair of AFB₁-N7-dG and AFB₁-Fapy-dG adducts occurs via the NER pathway [63,65], data establishing a role for BER in prokaryotes have been inconclusive [63,70]. Prior prokaryotic studies from the Essigmann laboratory had demonstrated an exclusive role for NER in aflatoxin adduct repair. These investigations were conducted in BER-proficient cells. However, Chetsanga and Frenette reported that the formamidopyrimidine DNA glycosylase, FPG, incised DNAs containing aflatoxin adducts [70]. Although activity against AFB₁-Fapy-dG adducts could fall within the FPG substrate range that includes 8-oxo-dG, Fapy-dG and Fapy-dA, our laboratories using site-specifically modified oligodeoxynucleotides have been unsuccessful in reproducing these findings (unpublished data).

7.1. NEIL1 incision of DNAs containing an AFB₁-Fapy-dG adduct

Even though our data for *E. coli* BER repair of aflatoxin adducts was negative, the possibility for such a role for BER in higher organisms has only recently been addressed. In this regard, the NEIL1 DNA glycosylase is predominately responsible for the initiation of

BER for a variety of Fapy adducts by catalyzing glycosyl bond scission to release the modified base and subsequently cleaving the phosphodiester backbone via combined β - and β,δ -elimination reactions [71–75]. Based on these observations, we initially investigated whether NEIL1 could incise DNA containing a site-specific AFB₁-Fapy-dG lesion [76]. Duplex DNAs (24-mer) containing either an AFB₁-Fapy-dG at position 12 or a known NEIL1 substrate thymine glycol (Tg), were constructed and incubated under single turnover kinetic conditions with excess NEIL1, since the release of NEIL1 from its products is known to be rate-limiting [71,77]. The product formation followed a single exponential rise with an observed excision rate constant of 0.17 ± 0.03 (average \pm SD) min^{-1} (Fig. 4) [76]. This rate constant is consistent with those previously reported for NEIL1 excision of 5-hydroxycytosine, 5-hydroxyuracil, and Tg (0.24, 0.14, and 1.3 min^{-1} , respectively) [78]. In excellent agreement with the prior literature, the observed rate constant for NEIL1-mediated incision of Tg was 1.35 ± 0.13 (average \pm SD) min^{-1} .

7.2. Increased AFB₁-Fapy-dG adduct accumulation in *Neil1*^{-/-} mouse livers relative to WT mice

The observed efficiency of NEIL1 catalyzed release of the AFB₁-Fapy-dG adducts was unanticipated, since the base modification stabilizes the melting temperature of a 12-mer duplex DNA by 15 °C [33,34]. This adduct also represents the largest DNA base modification reported as a substrate for any DNA glycosylase. To extend the in vitro biochemical analyses to an in vivo repair assay, newborn WT and *Neil1*^{-/-} mice [79,80], were injected with AFB₁ [76]. It was hypothesized that levels of AFB₁-Fapy-dG would be significantly lower in WT versus *Neil1*^{-/-} mice since the WT mice could repair these adducts via both the NER and BER pathways, while the *Neil1*^{-/-} mice would only repair this lesion via NER. Further, we hypothesized that the levels of cationic AFB₁-N7-dG adducts would not show difference between the two genotypes since NEIL1 does not recognize this lesion.

Newborn WT and *Neil1*^{-/-} mice (7 days old) were IP injected with AFB₁, livers harvested at 6 and 48 h post injection and DNA was extracted and analyzed by mass spectrometry. At the 6 h time point, both genotypes had approximately equal levels of the AFB₁-N7-dG and AFB₁-Fapy-dG adducts (Fig. 5) [76]. As anticipated, at the 48 h time point, the levels of AFB₁-N7-dG were significantly decreased in both genotypes, with these decreases attributable to a combination of spontaneous depurination, repair by NER, and conversion to the AFB₁-Fapy-dG adduct. In contrast to the levels of AFB₁-N7-dG, there was a significant difference in the amount of AFB₁-Fapy-dG adducts in WT versus *Neil1*^{-/-} mice (38.2 and 104.5 pmol/mg DNA, $p = 0.039$, respectively). These data implicate NEIL1 as a major contributor to initiation of repair of this lesion.

7.3. *Neil1*^{-/-} mice develop significantly higher frequencies of AFB₁-induced HCCs relative to WT mice

Since both the biochemical and in vivo adduct accumulation data suggested that NEIL1-initiated BER may contribute to the overall repair of the stable AFB₁-Fapy-dG adduct, it was hypothesized that *Neil1*^{-/-} mice would be more susceptible to AFB₁-induced carcinogenesis relative to WT C57Bl6J mice. WT and *Neil1*^{-/-} newborn pups were challenged with a single

IP injection of AFB₁ at 1.0 or 7.5 mg/kg in DMSO, with DMSO alone being used as a control. At 15 months post exposure, all mice were euthanized and examined for macroscopic tumors of the liver. All livers were fixed and prepared for serial sectioning and staining to determine tumor number and size [76]. No tumors were detected in any of the DMSO-injected controls. Consistent with prior literature [81], female mice of both genotypes were highly resistant to liver tumor induction, with only 2 out of 32 *Nei1*^{-/-} females developing tumors, while no tumors were observed in any WT females. All the following analyses are restricted to male mice. Based on glypican and reticulin stains, all tumors were classified as carcinomas. Liver cancers were observed in both the *Nei1*^{-/-} and WT males, albeit at greatly different frequencies and size distributions at both doses (Fig. 6A). For *Nei1*^{-/-} mice, the risk ratio of developing at least one tumor was calculated to be 3.15-fold greater than the corresponding risk of tumor development for WT mice (95% CI: 1.15–18.17; *p* = 0.020). It is interesting to note that the effect due to dose (7.5 mg/kg AFB₁ versus 1.0 mg/kg AFB₁) was comparable in size (risk ratio = 3.09; 95% CI: 1.57–7.06, *p* = 0.001) relative to the increase in tumor risk associated with genotype (Fig. 6B). The mean number of tumors per *Nei1*^{-/-} mouse versus WT was estimated to be 4.76-fold greater (95% CI: 1.36–30.03; *p* = 0.012). Similarly, the associated effect due to dose was comparable in the *Nei1*^{-/-} mice, with the mean number of tumors at 7.5 versus 1 mg/kg AFB₁ calculated to be 4.14 (95% CI: 1.77–10.56, *p* = 0.001) [76].

Since these data demonstrated that NEIL1-initiated repair contributed significantly to the reduction in AFB₁-induced HCCs in mice, analyses were performed to compare these data with a previous investigation that examined HCC formation in NER-deficient (*XPA*^{-/-}) mice following AFB₁ challenges [67]. Based on the reported numbers of mice with at least one tumor (Tables III-V [67]);, the risk ratios (*XPA*^{-/-} versus WT) were estimated to be 2.43-fold for DMSO vehicle alone, (*p* = 0.333), 1.53-fold at 0.6 mg/kg AFB₁) (*p* = 0.130) and 1.08-fold at 1.5 mg/kg AFB₁; (*p* = 0.669). The overall common risk ratio (adjusted for dose) was estimated to be 1.24 (95% CI: 0.91–1.79, *p* = 0.174) (Fig. 6C). Since *Nei1*^{-/-} mice had a 3.15-fold increased susceptibility, the 1.24-fold increase in the NER-deficient background suggests that NEIL1-initiated BER is more protective than NER.

8. Polymorphic variants of NEIL1

To explore whether the findings of increased susceptibility to aflatoxin-induced HCCs in *Nei1*-deficient mice could be extrapolated to increased tumor susceptibility in humans, it is necessary to determine if human polymorphic variants of NEIL1 have altered catalytic activities [82]. Initial biochemical studies characterized variants that were identified in individuals of Western European decent (S82C, G83D, C136R, and D252 N) with respect to glycosylase, β-elimination and δ-elimination activities. Using AP site-containing DNAs, WT, S82C and D252 N displayed qualitatively similar reactions, generating the expected β,δ-cleavage. However, although G83D incised AP DNA, the product was limited to the β-elimination reaction. Nicking activity of C136R was significantly reduced relative to any of the other enzymes and, like G83D, showed an uncoupling of the β,δ-elimination steps.

To characterize the overall substrate specificity of the WT human NEIL1 and its variants, GC/MS and LC/MS were used to assay release of damaged bases, using DNA samples that

had been previously exposed to ionizing radiation in N₂O-saturated buffered aqueous solution. Efficient excision of FapyAde and FapyGua from DNA by WT, S82C, and D252 N NEIL1 proteins was observed, while G83D and C136R exhibited no activity for any of these substrates. Collectively, these data suggested that two of the four polymorphic variants of NEIL1 representing individuals of European descent have severely diminished or abolished activities.

Although for many proteins, functional heterozygosity is frequently considered to be phenotypically neutral, the laboratory of Dr. Joann Sweasy (Yale University) has recently shown that expression of the G83D variant of NEIL1 induces an oncogenic phenotype in MCF10 A immortal human breast epithelial cells [83]. Expression of this variant in the presence of WT protein induced replication stress, genomic instability, and cellular transformation through a mechanism postulated to involve the masking of NEIL1 substrate DNA adducts at replication forks. These data suggest that repair of aflatoxin- and ROS-induced DNA damage could be blocked by catalytically-compromised, but correctly folded variants of NEIL1 that are capable of binding to specific DNA adducts. Additionally, we have previously demonstrated a significant phenotype in *Neil1*^{+/-} mice that showed intermediate (relative to WT and knockout) manifestations of the metabolic syndrome, including obesity, fatty liver disease, and elevated circulating leptin levels [79]. These data have significant implications for human health linking *hNEIL1* functional heterozygosity with increased susceptibility to AFB₁-associated HCCs.

We have also carried out systematic analyses of publicly-available sequence data bases for *NEIL1* variant allele frequencies including: 1) 1000 Genome, 2) ExAC that contains ~100,000 alleles, and 3) gnomAD (extension of the ExAC data base) which contains > 300,000 alleles that are distributed worldwide and contain ethnic and geographical details. Analyses of the gnomAD database for the previously characterized *NEIL1* variants (S82C, G83D, C136R, and D252N) showed that none of these variants were represented in populations of Eastern Asia or sub-Saharan Africa. In Eastern Asia, a total of 29 missense variants in the exomes of *NEIL1* were identified, with 3 of these, A51V, P68H, and G245R, present at > 0.1% frequencies. Supplementing these data, analyses of 1000 Genomes revealed 6 *NEIL1* missense variants, with P68H and G245R enriched in some populations. Although P68H is the most abundant variant when considering all Eastern Asia, the frequency varies considerably with ethnicities throughout the region, with the Kinh in Ho Chi Minh City, Vietnam at 4%. These analyses are further reinforced by a recent publication by Zhang et al. [62] in which exome sequencing or whole genome sequencing were carried out on 49 HCC patients from Qidong County, known for extremely high AFB exposures. The somatic mutation pattern in tumor tissues was dominated by an aflatoxin mutation signature (G to T transversions in specific sequence contexts). Analyses of the exons in *NEIL1* revealed that even though this was a very small cohort, all 3 common Eastern-Asian variants (A51V, P68H, and G245R) were identified in the Qidong cohort. Ongoing biochemical characterization of these, and additional variants, found in sub-Saharan Africa will be important in understanding if there is a role for NEIL1-initiated BER in limiting aflatoxin-initiated HCC formation.

A. paracitus	<i>Aspergillus paracitus</i>
AFB1	aflatoxin B ₁
AFB2	aflatoxin B ₂
AFG1	aflatoxin G ₁
AFG2	aflatoxin G ₂
AFB1-Fapy-dG	<i>trans</i> -89-dihydro-8-(2,6-diamino-4-oxo-3,4-dihydropyrimid-5-yl-formamido)-9-hydroxy aflatoxin B ₁
AFB1-N7-dG	<i>trans</i> -89-dihydro-8-(N7-guanyl)-9-hydroxy-aflatoxin B ₁ adduct
AP	abasic site
CYP	cytochrome p450
ds	double-stranded
Fapy A	46-diamino-5-formamidopyrimidine
Fapy G	26-diamno-4-hydroxy-5-formamidopyrimidine
HBsAg	hepatitis B surface antigen
HBV	hepatitis B virus
HCC	hepatocellular carcinoma
HCV	hepatitis C virus
MEF	mouse embryo fibroblasts
NMR	nuclear magnetic resonance
ss	single-stranded
WT	wild type

References

- [1]. Kensler TW, Roebuck BD, Wogan GN, Groopman JD, Aflatoxin: a 50-year odyssey of mechanistic and translational toxicology, *Toxicol. Sci* 120 (Suppl 1) (2011) S28–S48. [PubMed: 20881231]
- [2]. Kew MC, Aflatoxins as a cause of hepatocellular carcinoma, *J. Gastrointest. Liver Dis* 22 (2013) 305–310. [PubMed: 24078988]
- [3]. Sargeant K, Sheridan A, O’Kelly J, Carnaghan RBA, Toxicity associated with certain samples of groundnuts, *Nature* 192 (1961) 1096–1097.
- [4]. Lancaster MC, Jenkins FP, Philip JM, Toxicity associated with certain samples of groundnuts, *Nature* 192 (1961) 1095–1096.
- [5]. Blount WP, Turkey “x” disease, *Turkeys (J. Br. Turkey Fed.)* 9 (1961) 52–58.

- [6]. Williams JH, Phillips TD, Jolly PE, Stiles JK, Jolly CM, Aggarwal D, Human aflatoxicosis in developing countries: a review of toxicology, exposure, potential health consequences, and interventions, *Am. J. Clin. Nutr* 80 (2004) 1106–1122. [PubMed: 15531656]
- [7]. Chen JG, Egner PA, Ng D, Jacobson LP, Munoz A, Zhu YR, Qian GS, Wu F, Yuan JM, Groopman JD, et al., Reduced aflatoxin exposure presages decline in liver cancer mortality in an endemic region of china, *Cancer Prev. Res. Phila. (Phila)* 6 (2013) 1038–1045.
- [8]. Wu F, Mitchell NJ, Male D, Kensler TW, Reduced foodborne toxin exposure is a benefit of improving dietary diversity, *Toxicol. Sci* 141 (2014) 329–334. [PubMed: 25015663]
- [9]. Liao X, Liang Z, Strategy vaccination against hepatitis B in China, *Hum. Vaccin. Immunother* 11 (2015) 1534–1539. [PubMed: 25881006]
- [10]. Dohnal V, Wu Q, Kuca K, Metabolism of aflatoxins: key enzymes and inter-individual as well as interspecies differences, *Arch. Toxicol* 88 (2014) 1635–1644. [PubMed: 25027283]
- [11]. Kamdem LK, Meineke I, Godtel-Armbrust U, Brockmoller J, Wojnowski L, Dominant contribution of P450 3a4 to the hepatic carcinogenic activation of aflatoxin B₁, *Chem. Res. Toxicol* 19 (2006) 577–586. [PubMed: 16608170]
- [12]. Yamazaki H, Inui Y, Wrighton SA, Guengerich FP, Shimada T, Procarcinogen activation by cytochrome P450 3a4 and 3a5 expressed in *Escherichia coli* and by human liver microsomes, *Carcinogenesis* 16 (1995) 2167–2170. [PubMed: 7554070]
- [13]. Eaton DL, Bammler TK, Kelly EJ, Interindividual differences in response to chemoprotection against aflatoxin-induced hepatocarcinogenesis: implications for human biotransformation enzyme polymorphisms, *Adv. Exp. Med. Biol* 500 (2001) 559–576. [PubMed: 11764998]
- [14]. Gross-Steinmeyer K, Eaton DL, Dietary modulation of the biotransformation and genotoxicity of aflatoxin B(1), *Toxicology* 299 (2012) 69–79. [PubMed: 22640941]
- [15]. Johnson NM, Egner PA, Baxter VK, Sporn MB, Wible RS, Sutter TR, Groopman JD, Kensler TW, Roebuck BD, Complete protection against aflatoxin B(1)-induced liver cancer with a triterpenoid: DNA adduct dosimetry, molecular signature, and genotoxicity threshold, *Cancer Prev. Res. Phila. (Phila)* 7 (2014) 658–665.
- [16]. Livingstone MC, Johnson NM, Roebuck BD, Kensler TW, Groopman JD, Profound changes in miRNA expression during cancer initiation by aflatoxin B1 and their abrogation by the chemopreventive triterpenoid cddo-im, *Mol. Carcinog* 56 (2017) 2382–2390. [PubMed: 28218475]
- [17]. Williams DE, The rainbow trout liver cancer model: response to environmental chemicals and studies on promotion and chemoprevention, *Comp. Biochem. Physiol. C Toxicol. Pharmacol* 155 (2012) 121–127. [PubMed: 21704190]
- [18]. Slocum SL, Kensler TW, Nrf2: control of sensitivity to carcinogens, *Arch. Toxicol* 85 (2011) 273–284. [PubMed: 21369766]
- [19]. Smith LE, Prendergast AJ, Turner PC, Humphrey JH, Stoltzfus RJ, Aflatoxin exposure during pregnancy, maternal anemia, and adverse birth outcomes, *Am. J. Trop. Med. Hyg* 96 (2017) 770–776. [PubMed: 28500823]
- [20]. Sriwattanapong K, Slocum SL, Chawanthayatham S, Fedeles BI, Egner PA, Groopman JD, Satayavivad J, Croy RG, Essigmann JM, Editor's highlight: pregnancy alters aflatoxin B1 metabolism and increases DNA damage in mouse liver, *Toxicol. Sci* 160 (2017) 173–179. [PubMed: 28973694]
- [21]. Chawanthayatham S, Thiantanawat A, Egner PA, Groopman JD, Wogan GN, Croy RG, Essigmann JM, Prenatal exposure of mice to the human liver carcinogen aflatoxin B₁ reveals a critical window of susceptibility to genetic change, *Int. J. Cancer* 136 (2015) 1254–1262. [PubMed: 25070670]
- [22]. Li YW, Yang FC, Lu HQ, Zhang JS, Hepatocellular carcinoma and hepatitis B surface protein, *World J. Gastroenterol* 22 (2016) 1943–1952. [PubMed: 26877602]
- [23]. Chen T, Qian G, Fan C, Sun Y, Wang J, Lu P, Xue X, Wu Y, Zhang Q, Jin Y, et al., Qidong hepatitis B virus infection cohort: a 25-year prospective study in high risk area of primary liver cancer, *Hepatoma Res.* 4 (2018).
- [24]. Munoz A, Chen JG, Egner PA, Marshall ML, Johnson JL, Schneider MF, Lu JH, Zhu YR, Wang JB, Chen TY, et al., Predictive power of hepatitis B 1762t/1764a mutations in plasma for

- hepatocellular carcinoma risk in Qidong, China, *Carcinogenesis* 32 (2011) 860–865. [PubMed: 21474708]
- [25]. Liu ZM, Li LQ, Peng MH, Liu TW, Qin Z, Guo Y, Xiao KY, Ye XP, Mo XS, Qin X, et al., Hepatitis B virus infection contributes to oxidative stress in a population exposed to aflatoxin B₁ and high-risk for hepatocellular carcinoma, *Cancer Lett.* 263 (2008) 212–222. [PubMed: 18280645]
- [26]. Qi LN, Li LQ, Chen YY, Chen ZH, Bai T, Xiang BD, Qin X, Xiao KY, Peng MH, Liu ZM, et al., Genome-wide and differential proteomic analysis of hepatitis B virus and aflatoxin B₁ related hepatocellular carcinoma in Guangxi, China, *PLoS One* 8 (2013) e83465. [PubMed: 24391771]
- [27]. Chu YJ, Yang HI, Wu HC, Liu J, Wang LY, Lu SN, Lee MH, Jen CL, You SL, Santella RM, et al., Aflatoxin B₁ exposure increases the risk of cirrhosis and hepatocellular carcinoma in chronic hepatitis B virus carriers, *Int. J. Cancer* 141 (2017) 711–720. [PubMed: 28509392]
- [28]. Croy RG, Essigmann JM, Reinhold VN, Wogan GN, Identification of the principal aflatoxin B₁-DNA adduct formed in vivo in rat liver, *Proc. Natl. Acad. Sci. U. S. A* 75 (1978) 1745–1749. [PubMed: 273905]
- [29]. Essigmann JM, Croy RG, Nadzan AM, Busby WF Jr., Reinhold VN, Buchi G, Wogan GN, Structural identification of the major DNA adduct formed by aflatoxin B₁ in vitro, *Proc. Natl. Acad. Sci. U. S. A* 74 (1977) 1870–1874. [PubMed: 266709]
- [30]. Martin CN, Garner RC, Aflatoxin B₁-oxide generated by chemical or enzymic oxidation of aflatoxin B₁ causes guanine substitution in nucleic acids, *Nature* 267 (1977) 863–865. [PubMed: 895848]
- [31]. Croy RG, Wogan GN, Temporal patterns of covalent DNA adducts in rat liver after single and multiple doses of aflatoxin B₁, *Cancer Res.* 41 (1981) 197–203. [PubMed: 7448760]
- [32]. Coskun E, Jaruga P, Vartanian V, Erdem O, Egner PA, Groopman JD, Lloyd RS, Dizdaroglu M, Aflatoxin-guanine DNA adducts and oxidatively-induced DNA damage in aflatoxin-treated mice in vivo as measured by liquid chromatography-tandem mass spectrometry with isotope-dilution, *Chem. Res. Toxicol* (2018).
- [33]. Mao B, Hingerty BE, Broyde S, Patel DJ, Solution structure of the aminofluorene [AF]-external conformer of the anti-[AF]-c8-dG adduct opposite dC in a DNA duplex, *Biochemistry* 37 (1998) 95–106. [PubMed: 9425029]
- [34]. Brown KL, Deng JZ, Iyer RS, Iyer LG, Voehler MW, Stone MP, Harris CM, Harris TM, Unraveling the aflatoxin-Fapy conundrum: structural basis for differential replicative processing of isomeric forms of the formamidopyrimidine-type DNA adduct of aflatoxin B₁, *J. Am. Chem. Soc* 128 (2006) 15188–15199. [PubMed: 17117870]
- [35]. Foster PL, Eisenstadt E, Miller JH, Base substitution mutations induced by metabolically activated aflatoxin B₁, *Proc. Natl. Acad. Sci. U. S. A* 80 (1983) 2695–2698. [PubMed: 6405385]
- [36]. Smela ME, Currier SS, Bailey EA, Essigmann JM, The chemistry and biology of aflatoxin B(1): from mutational spectrometry to carcinogenesis, *Carcinogenesis* 22 (2001) 535–545. [PubMed: 11285186]
- [37]. Smela ME, Hamm ML, Henderson PT, Harris CM, Harris TM, Essigmann JM, The aflatoxin B(1) formamidopyrimidine adduct plays a major role in causing the types of mutations observed in human hepatocellular carcinoma, *Proc. Natl. Acad. Sci. U. S. A* 99 (2002) 6655–6660. [PubMed: 12011430]
- [38]. Bressac B, Kew M, Wands J, Ozturk M, Selective G to T mutations of p53 gene in hepatocellular carcinoma from southern Africa, *Nature* 350 (1991) 429–431. [PubMed: 1672732]
- [39]. Hsu IC, Metcalf RA, Sun T, Welsh JA, Wang NJ, Harris CC, Mutational hotspot in the p53 gene in human hepatocellular carcinomas, *Nature* 350 (1991) 427–428. [PubMed: 1849234]
- [40]. Scorsone KA, Zhou YZ, Butel JS, Slagle BL, P53 mutations cluster at codon 249 in hepatitis B virus-positive hepatocellular carcinomas from China, *Cancer Res.* 52 (1992) 1635–1638. [PubMed: 1311638]
- [41]. Fujimoto Y, Hampton LL, Wirth PJ, Wang NJ, Xie JP, Thorgeirsson SS, Alterations of tumor suppressor genes and allelic losses in human hepatocellular carcinomas in China, *Cancer Res.* 54 (1994) 281–285. [PubMed: 7903205]

- [42]. Hainaut P, Hernandez T, Robinson A, Rodriguez-Tome P, Flores T, Hollstein M, Harris CC, Montesano R, Iarc database of p53 gene mutations in human tumors and cell lines: updated compilation, revised formats and new visualisation tools, *Nucleic Acids Res.* 26 (1998) 205–213. [PubMed: 9399837]
- [43]. Kress S, Jahn UR, Buchmann A, Bannasch P, Schwarz M, P53 mutations in human hepatocellular carcinomas from Germany, *Cancer Res.* 52 (1992) 3220–3223. [PubMed: 1317262]
- [44]. Oda T, Tsuda H, Scarpa A, Sakamoto M, Hirohashi S, P53 gene mutation spectrum in hepatocellular carcinoma, *Cancer Res.* 52 (1992) 6358–6364. [PubMed: 1330291]
- [45]. Ozturk M, P53 mutation in hepatocellular carcinoma after aflatoxin exposure, *Lancet* 338 (1991) 1356–1359. [PubMed: 1682737]
- [46]. Besaratinia A, Kim SI, Hainaut P, Pfeifer GP, In vitro recapitulating of TP53 mutagenesis in hepatocellular carcinoma associated with dietary aflatoxin B₁ exposure, *Gastroenterology* 137 (1127–1137) (2009) 1137 e1121–1125.
- [47]. Dyaico MJ, Stuart GR, Tobal GM, de Boer JG, Glickman BW, Provost GS, Species-specific differences in hepatic mutant frequency and mutational spectrum among lambda/laci transgenic rats and mice following exposure to aflatoxin B₁, *Carcinogenesis* 17 (1996) 2347–2356. [PubMed: 8968048]
- [48]. Levy DD, Groopman JD, Lim SE, Seidman MM, Kraemer KH, Sequence specificity of aflatoxin B₁-induced mutations in a plasmid replicated in xeroderma pigmentosum and DNA repair proficient human cells, *Cancer Res.* 52 (1992) 5668–5673. [PubMed: 1394191]
- [49]. Lin YC, Li L, Makarova AV, Burgers PM, Stone MP, Lloyd RS, Molecular basis of aflatoxin-induced mutagenesis-role of the aflatoxin B₁-formamidopyrimidine adduct, *Carcinogenesis* 35 (2014) 1461–1468. [PubMed: 24398669]
- [50]. Lin YC, Li L, Makarova AV, Burgers PM, Stone MP, Lloyd RS, Error-prone replication bypass of the primary aflatoxin B₁ DNA adduct, AFB₁-N7-Gua, *J. Biol. Chem* 289 (2014) 18497–18506. [PubMed: 24838242]
- [51]. Lange SS, Bedford E, Reh S, Wittschieben JP, Carbajal S, Kusewitt DF, DiGiovanni J, Wood RD, Dual role for mammalian DNA polymerase zeta in maintaining genome stability and proliferative responses, *Proc. Natl. Acad. Sci. U. S. A* 110 (2013) E687–696. [PubMed: 23386725]
- [52]. Lange SS, Tomida J, Boulware KS, Bhetawal S, Wood RD, The polymerase activity of mammalian DNA pol zeta is specifically required for cell and embryonic viability, *PLoS Genet.* 12 (2016) e1005759. [PubMed: 26727495]
- [53]. Lange SS, Wittschieben JP, Wood RD, DNA polymerase zeta is required for proliferation of normal mammalian cells, *Nucleic Acids Res.* 40 (2012) 4473–4482. [PubMed: 22319213]
- [54]. Wittschieben JP, Patil V, Glushets V, Robinson LJ, Kusewitt DF, Wood RD, Loss of DNA polymerase zeta enhances spontaneous tumorigenesis, *Cancer Res.* 70 (2010) 2770–2778. [PubMed: 20215524]
- [55]. Wittschieben JP, Reshmi SC, Gollin SM, Wood RD, Loss of DNA polymerase zeta causes chromosomal instability in mammalian cells, *Cancer Res.* 66 (2006) 134–142. [PubMed: 16397225]
- [56]. Zander L, Bemark M, Immortalized mouse cell lines that lack a functional REV3 gene are hypersensitive to UV irradiation and cisplatin treatment, *DNA Repair (Amst.)* 3 (2004) 743–752. [PubMed: 15177183]
- [57]. Lin YC, Owen N, Minko IG, Lange SS, Li L, Stone MP, Wood RD, McCullough AK, Lloyd RS, DNA polymerase zeta limits chromosomal damage and promotes cell survival following aflatoxin exposure, *Proc. Natl. Acad. Sci. U. S. A* (2016) in press.
- [58]. Schulze K, Imbeaud S, Letouze E, Alexandrov LB, Calderaro J, Rebouissou S, Couchy G, Meiller C, Shinde J, Soysouvanh F, et al., Exome sequencing of hepatocellular carcinomas identifies new mutational signatures and potential therapeutic targets, *Nat. Genet* 47 (2015) 505–511. [PubMed: 25822088]
- [59]. Fedeles BI, Essigmann JM, Impact of DNA lesion repair, replication and formation on the mutational spectra of environmental carcinogens: aflatoxin B₁ as a case study, *DNA Repair (Amst.)* (2018).

- [60]. Chawanthayatham S, Valentine CC 3rd, Fedeles BI, Fox EJ, Loeb LA, Levine SS, Slocum SL, Wogan GN, Croy RG, Essigmann JM.) Mutational spectra of aflatoxin B₁ in vivo establish biomarkers of exposure for human hepatocellular carcinoma, *Proc. Natl. Acad. Sci. U. S. A* 114 (2017) E3101–E3109. [PubMed: 28351974]
- [61]. Huang MN, Yu W, Teoh WW, Ardin M, Jusakul A, Ng AWT, Boot A, Abedi-Ardekani B, Villar S, Myint SS, et al., Genome-scale mutational signatures of aflatoxin in cells, mice, and human tumors, *Genome Res.* 27 (2017) 1475–1486. [PubMed: 28739859]
- [62]. Zhang W, He H, Zang M, Wu Q, Zhao H, Lu LL, Ma P, Zheng H, Wang N, Zhang Y, et al., Genetic features of aflatoxin-associated hepatocellular carcinoma, *Gastroenterology* 153 (2017) 249–262 e242. [PubMed: 28363643]
- [63]. Alekseyev YO, Hamm ML, Essigmann JM, Aflatoxin B₁ formamidopyrimidine adducts are preferentially repaired by the nucleotide excision repair pathway in vivo, *Carcinogenesis* 25 (2004) 1045–1051. [PubMed: 14742311]
- [64]. Oleykowski CA, Mayernik JA, Lim SE, Groopman JD, Grossman L, Wogan GN, Yeung AT, Repair of aflatoxin B₁ DNA adducts by the UvrABC endonuclease of *Escherichia coli*, *J. Biol. Chem* 268 (1993) 7990–8002. [PubMed: 8463319]
- [65]. Leadon SA, Tyrrell RM, Cerutti PA, Excision repair of aflatoxin B₁-DNA adducts in human fibroblasts, *Cancer Res.* 41 (1981) 5125–5129. [PubMed: 6796265]
- [66]. Bedard LL, Alessi M, Davey S, Massey TE, Susceptibility to aflatoxin B₁-induced carcinogenesis correlates with tissue-specific differences in DNA repair activity in mouse and in rat, *Cancer Res.* 65 (2005) 1265–1270. [PubMed: 15735011]
- [67]. Takahashi Y, Nakatsuru Y, Zhang S, Shimizu Y, Kume H, Tanaka K, Ide F, Ishikawa T, Enhanced spontaneous and aflatoxin-induced liver tumorigenesis in xeroderma pigmentosum group A gene-deficient mice, *Carcinogenesis* 23 (2002) 627–633. [PubMed: 11960916]
- [68]. Long XD, Ma Y, Zhou YF, Yao JG, Ban FZ, Huang YZ, Huang BC, XpD codon 312 and 751 polymorphisms, and AFB₁ exposure, and hepatocellular carcinoma risk, *BMC Cancer* 9 (2009) 400. [PubMed: 19919686]
- [69]. Long XD, Ma Y, Zhou YF, Ma AM, Fu GH, Polymorphism in xeroderma pigmentosum complementation group C codon 939 and aflatoxin B₁-related hepatocellular carcinoma in the Guangxi population, *Hepatology* 52 (2010) 1301–1309. [PubMed: 20658464]
- [70]. Chetsanga CJ, Frenette GP, Excision of aflatoxin B₁-imidazole ring opened guanine adducts from DNA by formamidopyrimidine-DNA glycosylase, *Carcinogenesis* 4 (1983) 997–1000. [PubMed: 6409445]
- [71]. Hazra TK, Izumi T, Boldogh I, Imhoff B, Kow YW, Jaruga P, Dizdaroglu M, Mitra S, Identification and characterization of a human DNA glycosylase for repair of modified bases in oxidatively damaged DNA, *Proc. Natl. Acad. Sci. U. S. A* 99 (2002) 3523–3528. [PubMed: 11904416]
- [72]. Hu J, de Souza-Pinto NC, Haraguchi K, Hogue BA, Jaruga P, Greenberg MM, Dizdaroglu M, Bohr VA, Repair of formamidopyrimidines in DNA involves different glycosylases: role of the OGG1, NTH1, and NEIL1 enzymes, *J. Biol. Chem* 280 (2005) 40544–40551. [PubMed: 16221681]
- [73]. Morland I, Rolseth V, Luna L, Rognes T, Bjoras M, Seeberg E, Human DNA glycosylases of the bacterial Fpg/MutM superfamily: an alternative pathway for the repair of 8-oxoguanine and other oxidation products in DNA, *Nucleic Acids Res.* 30 (2002) 4926–4936. [PubMed: 12433996]
- [74]. Chan MK, Ocampo-Hafalla MT, Vartanian V, Jaruga P, Kirkali G, Koenig KL, Brown S, Lloyd RS, Dizdaroglu M, Teebor GW, Targeted deletion of the genes encoding NTH1 and NEIL1 DNA N-glycosylases reveals the existence of novel carcinogenic oxidative damage to DNA, *DNA Repair (Amst.)* 8 (2009) 786–794. [PubMed: 19346169]
- [75]. Jaruga P, Birincioglu M, Rosenquist TA, Dizdaroglu M, Mouse NEIL1 protein is specific for excision of 2,6-diamino-4-hydroxy-5-formamidopyrimidine and 4,6-diamino-5-formamidopyrimidine from oxidatively damaged DNA, *Biochemistry* 43 (2004) 15909–15914. [PubMed: 15595846]

- [76]. Vartanian V, Minko IG, Chawanthayatham S, Egner PA, Lin YC, Earley LF, Makar R, Eng JR, Camp MT, Li L, et al., NEIL1 protects against aflatoxin-induced hepatocellular carcinoma in mice, *Proc. Natl. Acad. Sci. U. S. A* 114 (2017) 4207–4212. [PubMed: 28373545]
- [77]. Wallace SS, Bandaru V, Kathe SD, Bond JP, The enigma of endonuclease VIII, *DNA Repair (Amst)* 2 (2003) 441–453. [PubMed: 12713806]
- [78]. Vik ES, Alseth I, Forsbring M, Helle IH, Morland I, Luna L, Bjoras M, Dalhus B, Biochemical mapping of human NEIL1 DNA glycosylase and AP lyase activities, *DNA Repair (Amst.)* 11 (2012) 766–773. [PubMed: 22858590]
- [79]. Vartanian V, Lowell B, Minko IG, Wood TG, Ceci JD, George S, Ballinger SW, Corless CL, McCullough AK, Lloyd RS, The metabolic syndrome resulting from a knockout of the Neil1 DNA glycosylase, *Proc. Natl. Acad. Sci. U. S. A* 103 (2006) 1864–1869. [PubMed: 16446448]
- [80]. Sampath H, Batra AK, Vartanian V, Carmical JR, Prusak D, King IB, Lowell B, Earley LF, Wood TG, Marks DL, et al., Variable penetrance of metabolic phenotypes and development of high-fat diet-induced adiposity in Neil1-deficient mice, *Am. J. Physiol. Endocrinol. Metab* 300 (2011) E724–734. [PubMed: 21285402]
- [81]. Vesselinovitch SD, Mihailovich N, Wogan GN, Lombard LS, Rao KV, Aflatoxin B₁, a hepatocarcinogen in the infant mouse, *Cancer Res.* 32 (1972) 2289–2291. [PubMed: 4343225]
- [82]. Roy LM, Jaruga P, Wood TG, McCullough AK, Dizdaroglu M, Lloyd RS, Human polymorphic variants of the Neil1 DNA glycosylase, *J. Biol. Chem* 282 (2007) 15790–15798. [PubMed: 17389588]
- [83]. Galick HA, Marsden CG, Kathe S, Dragon JA, Volk L, Nemecek AA, Wallace SS, Prakash A, Doublet S, Sweasy JB, The Neil1 G83D germline DNA glycosylase variant induces genomic instability and cellular transformation, *Oncotarget* 8 (2017) 85883–85895. [PubMed: 29156764]

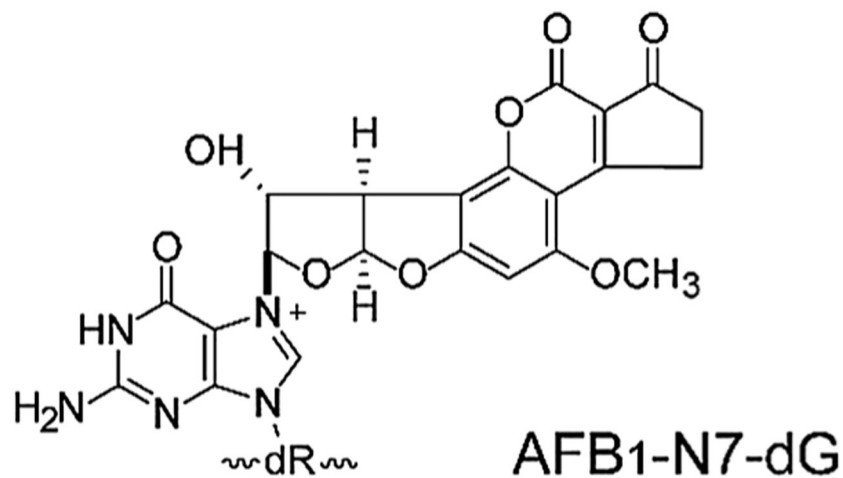
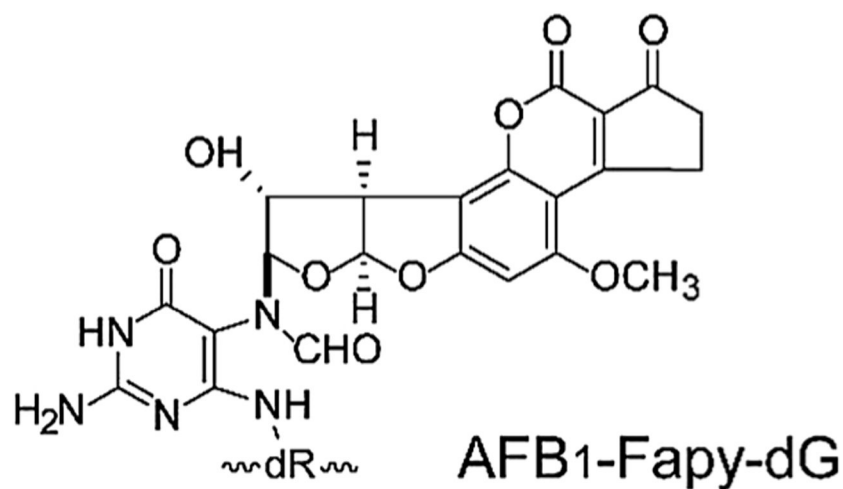
A**B**

Fig. 1. DNA Adduct Structures.

(A) Structure of the AFB₁-N7-dG adduct. (B) Structure of the AFB₁-Fapy-dG adduct.

[Reproduced from [76] Fig. 1].

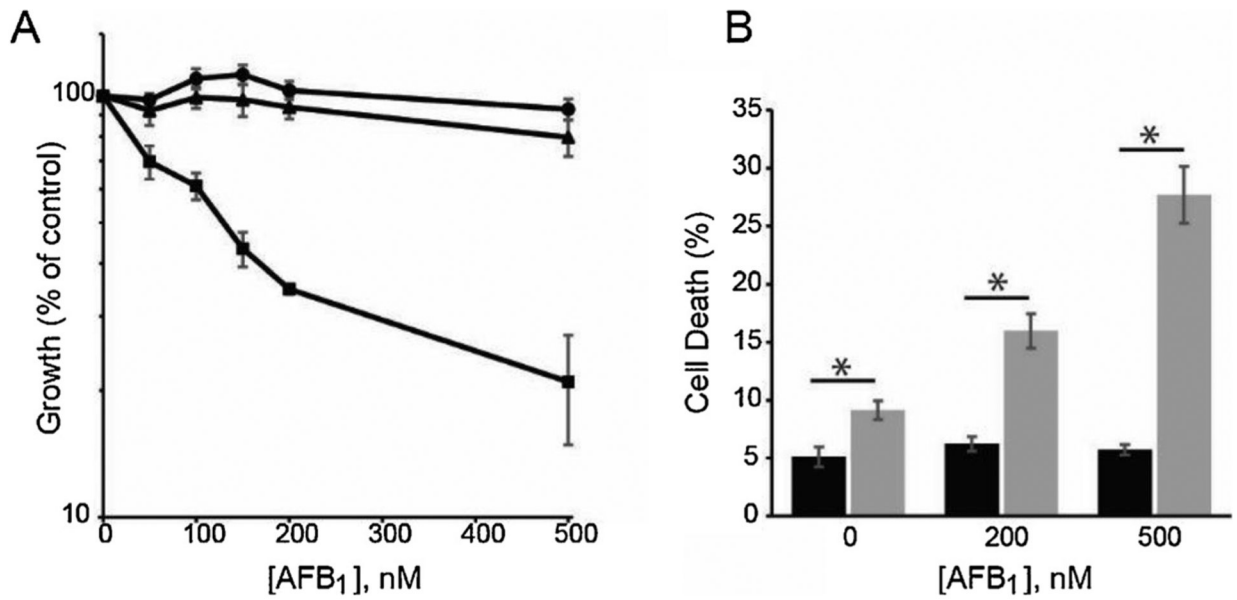


Fig. 2. Mammalian pol ζ protects against AFB₁-induced cytotoxicity.

(A) Growth inhibition in *Rev3L*^{+/+} (circles), *Rev3L*^{-/-} (squares), and *Rev3L*^{-/-} + *hRev3L* (triangles) MEFs was determined 48 h after AFB₁ treatment by measuring cellular ATP. (B) Quantification of total cell death (Annexin V+/PI-, Annexin V-/PI+ and Annexin V+/PI+) in *Rev3L*^{+/+} (black bars) and *Rev3L*^{-/-} (gray bars) MEFs following AFB₁ treatment. Data represent mean \pm SEM from three independent experiments. * $P < 0.05$ by unpaired two-tailed t -test with unequal variances. [Reproduced from [57], Fig. 1, Panels A and B].

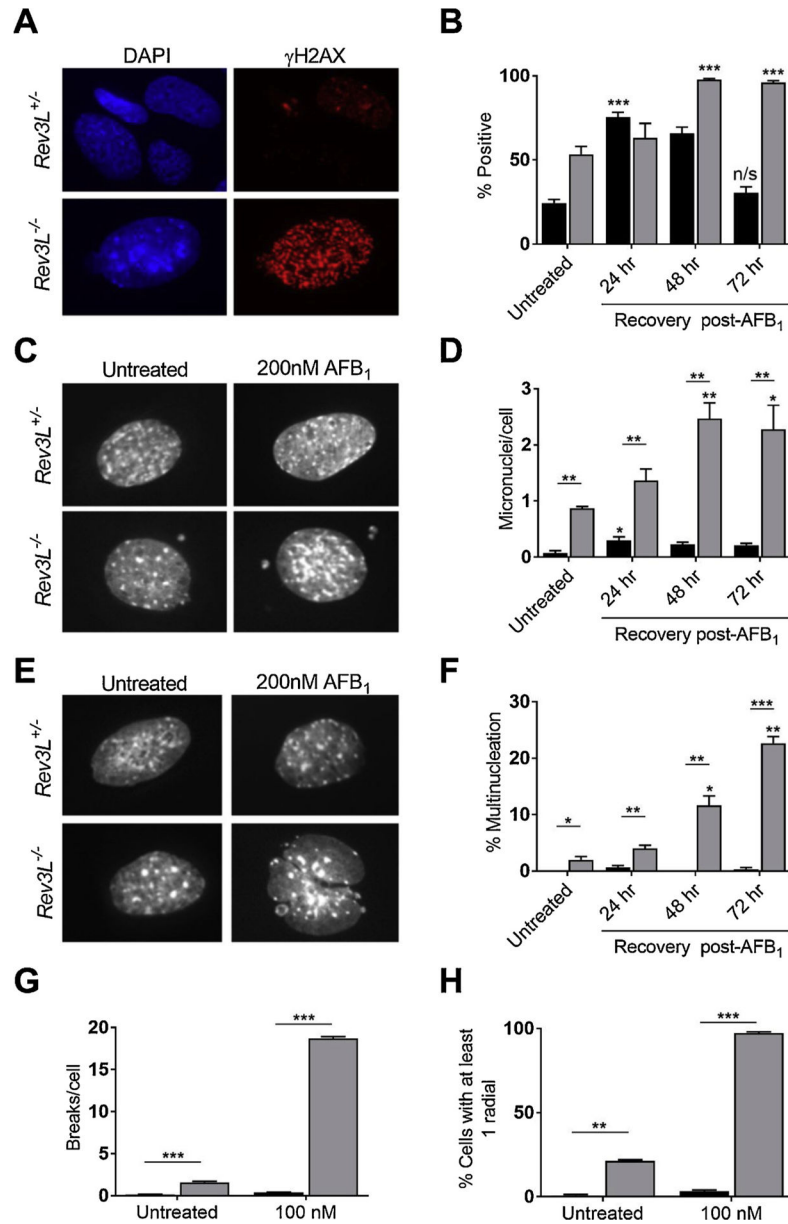


Fig. 3. Genome instability generated by AFB₁ exposures in pol ζ-deficient cells.

(A) DSB formation was assessed by measuring the accumulation and resolution of γ -H2AX foci in response to 200 nM AFB₁ +S9 for 1.5 h. Representative images of γ -H2AX foci in *Rev3L*^{+/-} (top) and *Rev3L*^{-/-} (bottom) cells at 72 h post-exposure. (B) Quantification of γ -H2AX foci over time in response to AFB₁ exposure. (C–F) Genome instability in interphase cells was assessed by micronuclei formation and the appearance of multinucleated cells. Representative images (C) and quantification (D) of micronuclei. Representative images (E) and quantification (F) of multinucleated cells. (G–H) Following a 1.5 h AFB₁ exposure, genome instability in metaphase cells was assessed by chromosome breakage analyses after 48 h recovery. Quantification of chromatid breaks (G) and chromosomal radials (H) reflecting aberrant DNA repair. Data represent the mean \pm SEM from three independent experiments. * $p < 0.05$, ** $p < 0.01$, *** $p < 0.001$ by unpaired two-tailed t-test with

unequal variances. The p-values above bars are comparing treated and untreated cells; p-values between bars are comparing between cell lines. n/s = not significant. Black bars = *Rev3L^{+/-}*; Gray bars = *Rev3L^{-/-}*. [Reproduced from [57], Fig. 3].

5' -ACCACTACTAT**X**ATTCATAACAAC-3'
 3' -TGGTGATGATACTAAGTATTGTTG-5'

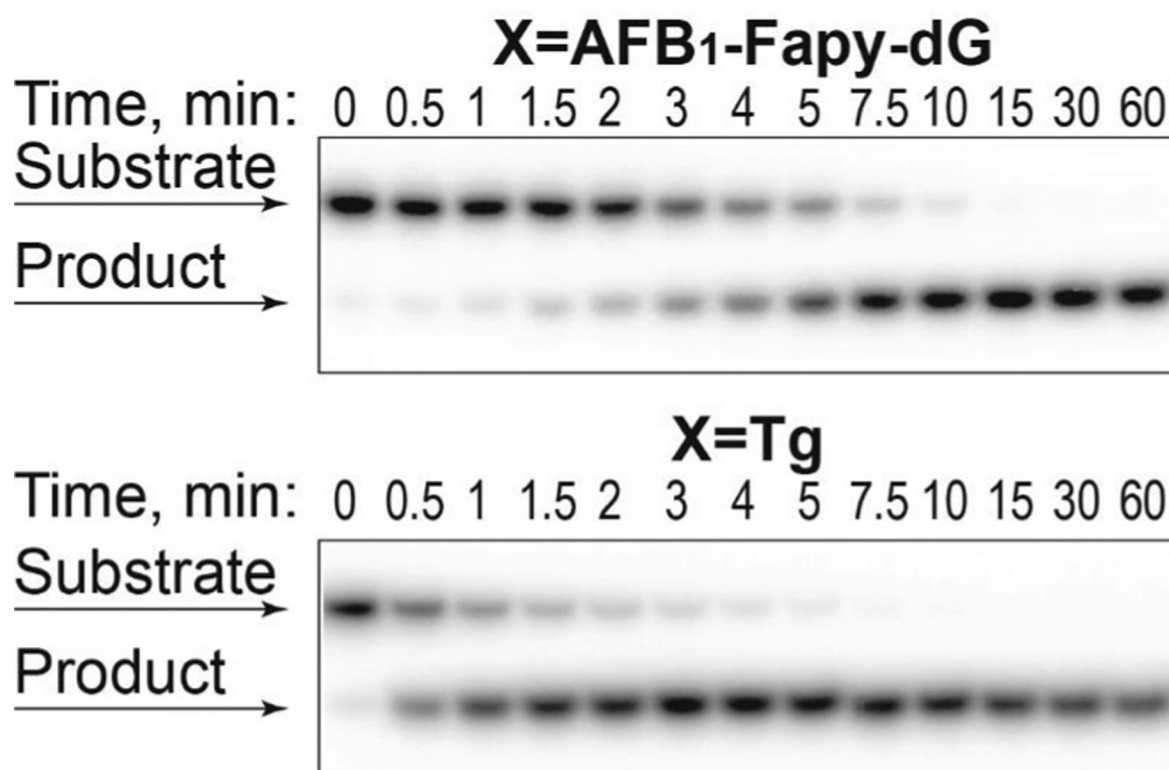


Fig. 4. NEIL1-catalyzed incision of DNA containing an AFB₁-Fapy-dG adduct. ³²P-labeled oligodeoxynucleotides (20 nM) containing either AFB₁-Fapy-dG in fully duplex DNA (A) or Tg in fully duplex DNA (B) were incubated with hNEIL1 (230 nM). The aliquots were removed at the indicated times, and following separation by gel-electrophoresis, DNA was visualized using a phosphor screen and Personal Molecular Imager™ System (Bio-Rad). The representative gel images are shown. [Reproduced from [76], Fig. 2].

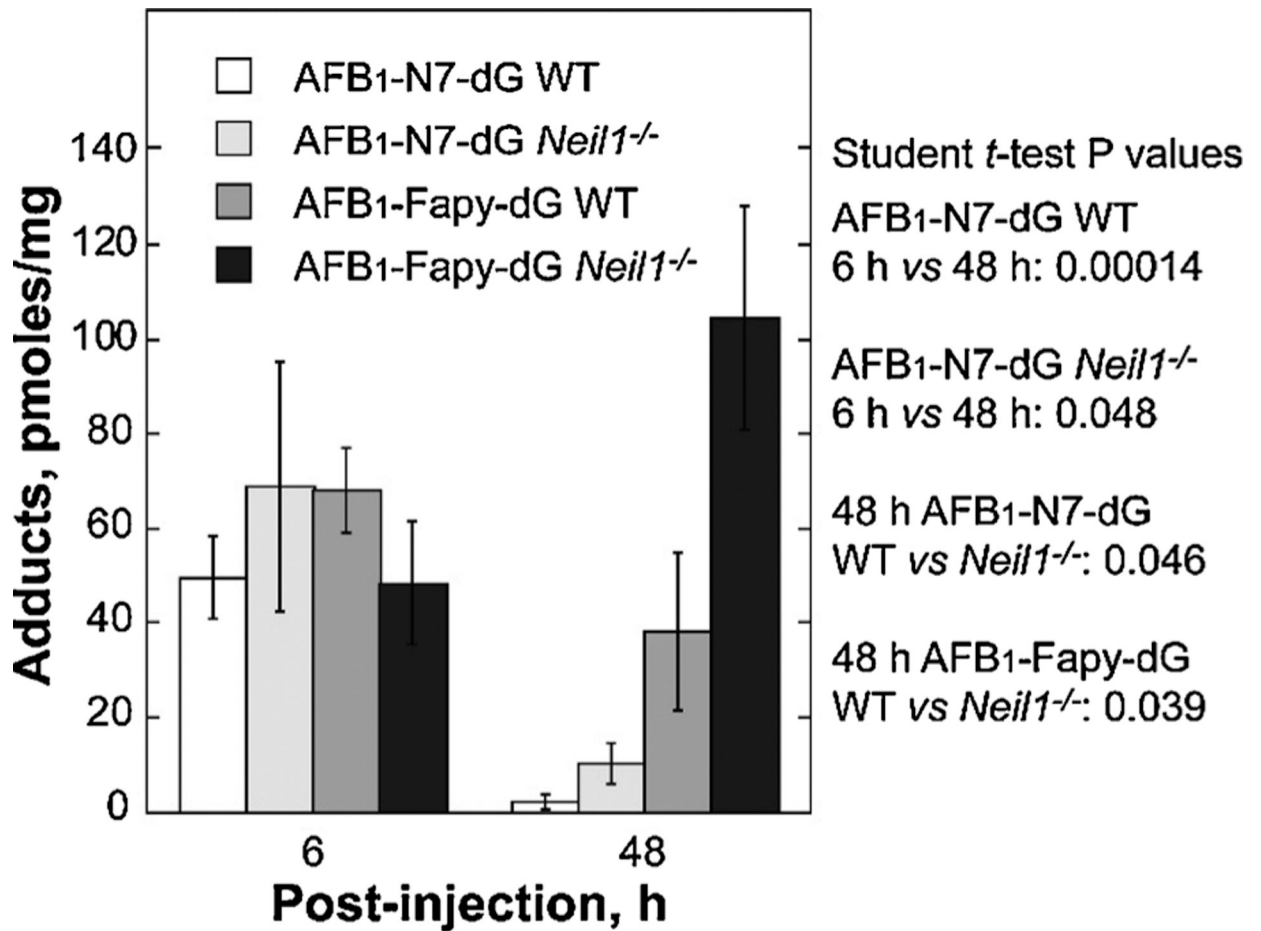


Fig. 5. Levels of AFB₁-induced DNA adducts in liver DNA from of WT and *Neil1*^{-/-} mice following AFB₁ IP injection.

Neil1^{-/-} and control WT mice (6 day old pups) were injected with 10 mM AFB₁ in DMSO at a dose of 3.5 mg/kg. Livers were harvested at 6 and 48 h post-injection, immediately frozen in liquid nitrogen, and DNA isolated for AFB₁ adduct analysis. Following acid hydrolysis, internal ¹⁵N₅-guanine-derived standards were added to permit quantitative analysis by isotope dilution mass spectrometry for both AFB₁-N7-dG and AFB₁-Fapy-dG. Adducts were separated by ultra-performance liquid-chromatography mass spectrometry. The protonated parent ion of the AFB₁-N7-dG adduct (*m/z* 480.1) was selected and subjected to collision-induced fragmentation producing a *m/z* 152 product ion that was monitored to quantify adduct levels. The AFB₁-Fapy-dG adduct was measured by selection of the *m/z* 498 parent ion and monitoring the collision-induced product ion *m/z* 452.29. [Reproduced from [76], Fig. 2].

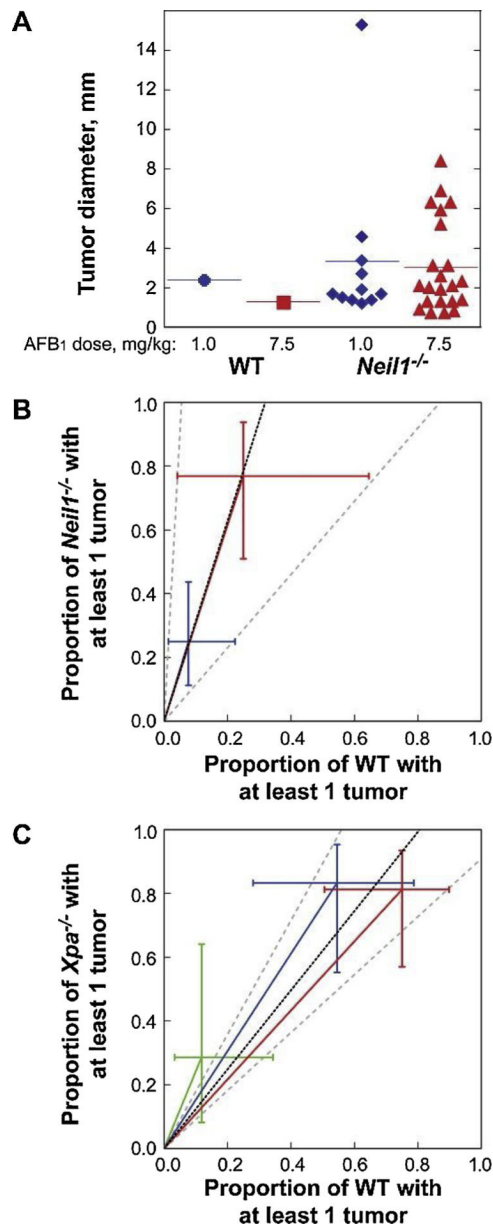


Fig. 6. AFB₁-induced carcinogenesis in *Neil1*^{-/-} and *XPA*^{-/-} mice. (A) The individual diameter of liver tumors observed in AFB₁-injected WT and *Neil1*^{-/-} mice. Relative AFB₁-induced tumor risk analysis in (B) *Neil1*^{-/-} mice, with data illustrated by blue and red symbols representing AFB₁ doses of 1.0 and 7.5 mg/kg respectively and (C) *XPA*^{-/-} mice, with data illustrated by green, blue and red symbols representing AFB₁ doses of 0, 0.6 and 1.5 mg/kg, respectively. [Reproduced from [76], Fig. 4].

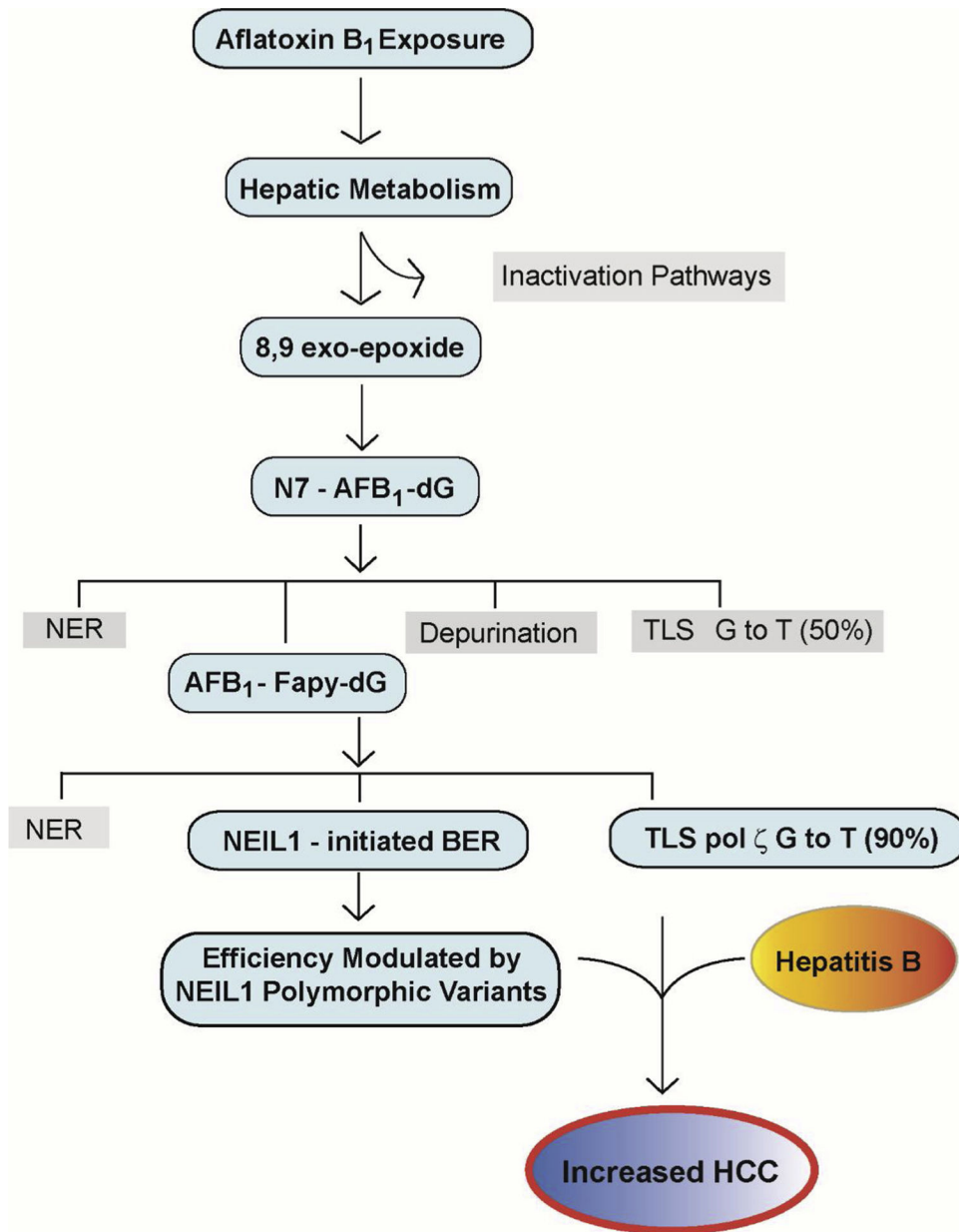


Fig. 7. Key Steps in Modulating Aflatoxin B₁ Mutagenesis and Carcinogenesis.

Following ingestion of foods that are contaminated with *Aspergillus flavus*, hepatic metabolism shuttles AFB₁ into pathways that are either biologically harmless (Inactivation Pathways) or biologically activated as the 8,9 *exo*-epoxide for subsequent reaction at N7-guanine. Although the product of this reaction, the N7- AFB₁-dG adduct is relatively short lived, it can be repaired by NER, undergo depurination with repair completed via BER, replicated by an error-prone mechanism yielding ~50% G to T transversions, or hydrolyzed to the long-lived AFB₁-Fapy-dG adduct. This adduct is subject to repair via NER, replicated in a highly error-prone mechanism by DNA polymerase ζ, yielding ~90% G to T transversions and ~7% G to A transitions, or repaired *via* BER initiated by NEIL1. Catalytically-inactive, but accurately folded, polymorphic variants of NEIL1 are

hypothesized to interfere with normal repair and thus, lead to increased numbers of unrepaired sites that contribute to overall genetic instability. It is this combination of decreased repair, error-prone replication, and hepatitis B infection and chronic inflammation that leads to increased risk of HCC formation.

Author Manuscript

Author Manuscript

Author Manuscript

Author Manuscript